arXiv:1406.5707v2 [cond-mat.quant-gas] 11 Sep 2014

Quantum Criticality of one-dimensional multicomponent Fermi Gas with Strongly Attractive Interaction

Peng He[1], Yuzhu Jiang[2], Xiwen Guan[2,3], and Jinyu He[4]

1 *Beijing National Laboratory for Condensed Matter Physics, Institute of Physics, Chinese Academy of Sciences, Beijing 100190, P. R. China*

2 *State Key Laboratory of Magnetic Resonance and Atomic and Molecular Physics, Wuhan Institute of Physics and Mathematics, Chinese Academy of Sciences, Wuhan 430071, China*

3 *Department of Theoretical Physics, Research School of Physics and Engineering, Australian National University, Canberra ACT 0200, Australia and*

4 *Dezhou University, Dezhou 253023, China*

Abstract

Quantum criticality of strongly attractive Fermi gas with $SU(3)$ symmetry in one dimension is studied via the thermodynamic Bethe ansatz (TBA) equations. The phase transitions driven by the chemical potential μ, effective magnetic field H_1, H_2 (chemical potential biases) are analyzed at the quantum criticality. The phase diagram and critical fields are analytically determined by the thermodynamic Bethe ansatz equations in zero temperature limit. High accurate equations of state, scaling functions are also obtained analytically for the strong interacting gases. The dynamic exponent $z = 2$ and correlation length exponent $\nu = 1/2$ read off the universal scaling form. It turns out that the quantum criticality of the three-component gases involves a sudden change of density of states of one cluster state, two or three cluster states. In general, this method can be adapted to deal with the quantum criticality of multi-component Fermi gases with $SU(N)$ symmetry.

PACS numbers: 03.75.Ss, 03.75.Hh, 02.30.IK, 05.30.Fk

I. INTRODUCTION

Quantum phase transition occurs between different phases of matter by varying the driving parameter, such as magnetic field, chemical potential or interaction strength, at zero temperature. It is driven by quantum fluctuations associated with the Heisenberg uncertainty principle rather than by thermodynamic fluctuations [1]. In critical regime, i.e., the regime near the critical point, the problem becomes much more difficult because quantum fluctuation and thermodynamic fluctuation couple strongly with each other. Novel critical phenomena associated with rich symmetries are also emergent with respect to the quantum phase transition. For example, one-dimensional(1D) quantum Ising chain with transverse field exhibits E_8 symmetry near the critical point [2].

However, most of the traditional methods fails in the quantum critical regime because the fluctuation is very strong and cannot be neglected. Therefore, many new methods are proposed in literature, such as the effective field theory [1, 3], renormalization group approach [4, 5], field theory [6] and AdS/CFT correspondence [7–9]. Recently, Zhou and Ho suggested a practicable way to map out the $T = 0$ phase diagram of the bulk systems from the density profile of a trapped gas at low temperatures [10, 11]. This opens the research on quantum criticality in 1D integrable systems for which the equation of state can be systematically derived in terms of polylogarithm function via thermodynamic Bethe ansatz (TBA) method in the strong coupling limit [12–15]. The quantum criticality of 1D strongly attractive spin 1/2 Fermi gas and the Lieb-Liniger gas were investigated via TBA method [24, 25]. The equation of state obtained analytically from the TBA equations provides rich insight into critical behavior. This method has been applied to the Bose-Fermi mixture and quantum gases in an harmonic trap [26, 27], see review [28].

Beyond spin-1/2 Fermi gas, the low temperature thermodynamics of multi-component, especially three-component Fermi gas were studied for various limited cases [15, 29–32]. The phase diagrams at zero temperature were investigated via both analytical and numerical methods [29, 32]. The finite temperature properties, Tomonaga-Luttinger liquid physics and equation of state were analytically studied as well [15]. For three-component Fermi gas, there exist three kinds of composite particles in attractive regime, which form the normal Fermi gas of single fermions and quantum gases of pairs (two-particle bound state) and trions (three-particle bound state) as well as their mixtures. In contrast, the 1D spin-1

bosons with repulsive density-density and antiferromagnetic spin-exchange interactions [16–19] exhibit either a spin-singlet paired ground state or a fully polarized ferromagnetic ground state. These rich phase diagrams provide novel quantum criticality of the system towards to understanding critical behavior of multicomponent fermions. The multi-component Fermi gases have been attracted a considerable attention from a wide range of physics, see a recent review [20]. In particular, recent experiment with ^{171}Yb atoms with nuclear spin $I = 1/2$ and ^{173}Yb atoms with $I = 5/2$ [21] realized the model of Fermi mixture with $SU(2) \otimes SU(6)$ symmetry. Realizations of the $SU(6)$ Mott-insulator state with ultracold fermions of ^{173}Yb atoms [22] and the 1D multicomponent fermions of ^{173}Yb [23] open to further study of ultracold atoms with large spin symmetries.

In this paper, we obtain analytically higher precision equation of states which facilitates work out quantum criticality of the model. The phase boundaries and the scaling functions of density n and compressibility κ are derived in various choices of two external magnetic fields. By controlling two external fields, the quantum criticality of the model involves different cluster states of different sizes. This nature can be generalized to multicomponent Fermi gases. We further show that the critical behavior of homogeneous systems can be mapped out from the density profile of inhomogeneous systems and the phase boundary at absolute zero temperature can also be determined from the finite temperature properties. In recent years, the experimental simulation with 1D systems develop fast [33]. Our result pave a way to experimental observation of quantum criticality of multicomponent Fermi gases.

This paper is organized as follows. In section II, high precision equation of state is derived in terms of polylogarithm function from the TBA equations. In section III, the phase boundaries of all phases are given analytically by large-c approximation from the TBA equations. In section IV, we studied the quantum criticality of the system at the phase transitions from vacuum to trion and from the mixture of unpaired fermions and pairs to the mixture of three kinds of composite particles, i.e. trions, pairs and single fermions. In section V, we give a brief summary and discussion.

II. THE MODEL, TBA EQUATIONS AND EQUATIONS OF STATES

The many-body Hamiltonian of a 1D Fermi gas with attractive δ-function interaction is [34–36]

$$\mathcal{H}_0 = -\frac{\hbar^2}{2m}\sum_{i=1}^{N}\frac{\partial^2}{\partial x_i^2} + g_{1D}\sum_{1\le i<j\le N}\delta(x_i - x_j) + E_z. \tag{1}$$

where m is the mass of each fermions in this system and the Zeeman energy is $E_z = \sum_{i=1}^{3} N^i \epsilon_Z^i$ here. [15] The contact interaction strength g_{1D} is spin independent and exists only between fermions with different hyperfine states. It is negative for attractive interaction and positive for repulsive interaction. In the system we considered, there are three possible hyperfine levels ($|1\rangle$, $|2\rangle$, and $|3\rangle$). The periodic boundary condition is applied here. For simplicity, we set $\hbar = 2m = 1$ and they can be restored when necessary. In experiments, the scattering length between the hyperfine states can be tuned via the broad Feshbach resonance. The sublevels can form $SU(3)$ symmetry under a proper choice of scattering length in each channels.

The Bethe ansatz equations and TBA equations for attractive case are shown in our earlier work [15]. In low temperature, the contribution of spin fluctuation is suppressed by the strong magnetic field and can be analytically calculated through our approach. The full

TBA equations read

$$
\begin{aligned}
\varepsilon_1 &= k^2 - \mu - H_1 + Ta_1 * \ln(1+e^{-\varepsilon_2/T}) \\
&+ Ta_2 * \ln(1+e^{-\varepsilon_3/T}) - T\sum_n a_n * \ln(1+\xi_n^{-1}), \qquad (2)\\
\varepsilon_2 &= 2k^2 - \frac{c^2}{2} - 2\mu - H_2 + Ta_1 * \ln(1+e^{-\varepsilon_1/T}) \\
&+ Ta_2 * \ln(1+e^{-\varepsilon_2/T}) + T(a_1+a_3) * \ln(1+e^{-\varepsilon_3/T}) \\
&- T\sum_n a_n * \ln(1+\zeta_n^{-1}), \qquad (3)\\
\varepsilon_3 &= 3k^2 - 2c^2 - 3\mu + Ta_2 * \ln(1+e^{-\varepsilon_1/T}) \\
&+ T(a_1+a_3) * \ln(1+e^{-\varepsilon_2/T}) + T(a_2+a_4) * \ln(1+e^{-\varepsilon_3/T}), \qquad (4)\\
\ln\xi_n &= \frac{n(2H_1-H_2)}{T} + a_n * \ln(1+e^{-\varepsilon_1/T}) \\
&+ \sum_m T_{mn} * \ln(1+\xi_m^{-1}) - \sum_m S_{mn} * \ln(1+\zeta_m^{-1}), \qquad (5)\\
\ln\zeta_n &= \frac{n(2H_2-H_1)}{T} + a_n * \ln(1+e^{-\varepsilon_2/T}) \\
&+ \sum_m T_{mn} * \ln(1+\zeta_m^{-1}) - \sum_m S_{mn} * \ln(1+\xi_m^{-1}), \qquad (6)
\end{aligned}
$$

Here the quantity $a_m(x) = \frac{1}{2\pi}\frac{m|c|}{(mc/2)^2+x^2}$, and $*$ denotes the convolution, $(a*b)(x) = \int a(x-y)b(y)dy$. The Eqs. (2)-(4) are the dressed energies of single atoms ε_1 and dressed energies of two- and three-body cluster states ε_2 and ε_3 in charge sector. Here the two-body cluster state involves the two-body bound states $\{\lambda_j \pm ic/2\}, j = 1,\ldots,M_2$ and the three-body bound states $\{\lambda_j \pm ic, \lambda_j\}, j = 1,\ldots,M_3$, where M_2 and M_3 are the numbers of two-body bound states and three-body bound states, respectively [15]. They are determined by external fields, chemical potential, interaction between different clusters and spin wave fluctuations. The (5)-(6) characterize spin wave fluctuations. The effective chemical potentials H_i are determined by the chemical potential μ and the Zeeman energies [32]. In very low temperatures, the contributions of spin flipping are exponential small in strong coupling

regimes and therefore they can be neglected and thus we have

$$\begin{aligned}
\varepsilon_1(k) &= k^2-\mu-H_1+Ta_1*\ln(1+e^{-\varepsilon_2(k)/T})+Ta_2*\ln(1+e^{-\varepsilon_3(k)/T}),\\
\varepsilon_2(k) &= 2k^2-2\mu-\frac{c^2}{2}-H_2+Ta_1*\ln(1+e^{-\varepsilon_1(k)/T})+Ta_2*\ln(1+e^{-\varepsilon_2(k)/T})\\
&\quad +T(a_1+a_3)*\ln(1+e^{-\varepsilon_3(k)/T}),\\
\varepsilon_3(k) &= 3k^2-3\mu-2c^2+Ta_2*\ln(1+e^{-\varepsilon_1(k)/T})+T(a_1+a_3)*\ln(1+e^{-\varepsilon_2(k)/T})\\
&\quad +T(a_2+a_4)*\ln(1+e^{-\varepsilon_3(k)/T}).
\end{aligned}\tag{7}$$

In the thermodynamic limit, the pressure p is defined as the Gibbs energy per length [15], which includes three parts, p_1, p_2 and p_3 and can be expressed in the general form

$$p_r=\frac{rT}{2\pi}\int dk\ln\left(1+e^{-\varepsilon_r(k)/T}\right),\tag{8}$$

where effective masses $r=1,2,3$, which stand for the unpaired fermions, pairs, and trions, respectively. Here we have already set the Boltzmann constant $k_B=1$.

The TBA equations (7) are expressed in terms of the dressed energies $\varepsilon_1(k)$, $\varepsilon_2(k)$ and $\varepsilon_3(k)$ for unpaired fermions, pairs and trions, respectively. The dressed energies depend only on the chemical potential μ and the external fields H_1 and H_2 when the spin terms are neglected in low temperature. The TBA equations play the central role in the investigation of thermodynamic properties of exactly solvable models at finite temperature. They also provide a convenient formalism to analyze quantum phase transitions and magnetic effects in the presence of external fields at zero temperature [37].

In the strong coupling limit, the convolution integrals in TBA equations (7) can be simplified and expressed in terms of the pressure (13) [15]

$$\varepsilon_r(k)\ \approx\ r\,k^2-A^{(r)},\qquad r=1,\,2,\,3,\tag{9}$$

where $A^{(r)}$ can be written as

$$\begin{aligned}
A^{(1)} &= \mu+H_1-\frac{2}{|c|}p_2-\frac{2}{3|c|}p_3+\frac{1}{4|c|^3}Y^{(2)}_{\frac{5}{2}}+\frac{1}{9|c|^3}Y^{(3)}_{\frac{5}{2}},\\
A^{(2)} &= 2\mu+\frac{1}{2}c^2+H_2-\frac{4}{|c|}p_1-\frac{1}{|c|}p_2-\frac{16}{9|c|}p_3+\frac{8}{|c|^3}Y^{(1)}_{\frac{5}{2}}+\frac{1}{4|c|^3}Y^{(2)}_{\frac{5}{2}}+\frac{224}{243|c|^3}Y^{(3)}_{\frac{5}{2}},\\
A^{(3)} &= 3\mu+2c^2-\frac{2}{|c|}p_1-\frac{8}{3|c|}p_2-\frac{1}{|c|}p_3+\frac{1}{2|c|^3}Y^{(1)}_{\frac{5}{2}}+\frac{28}{27|c|^3}Y^{(2)}_{\frac{5}{2}}+\frac{1}{16|c|^3}Y^{(3)}_{\frac{5}{2}}.
\end{aligned}\tag{10}$$

For simplicity, define

$$Y^{(r)}_a=-\sqrt{\frac{r}{4\pi}}T^a\mathrm{Li}_a\left(-e^{A^{(r)}/T}\right),\tag{11}$$

where the effective masses $r = 1, 2, 3$. The polylogarithm function is defined as $\mathrm{Li}_n(x) = \sum_{k=1}^{\infty} \frac{x^k}{k^n}$. Hence the pressure (13) can be expressed in terms of polylogarithm function after integration by parts

$$\begin{aligned}
p_1 &= Y_{\frac{3}{2}}^{(1)} \left[1 + \frac{4p_2}{|c|^3} + \frac{p_3}{3|c|^3} \right] \\
&= Y_{\frac{3}{2}}^{(1)} \left[1 + \frac{4}{|c|^3} Y_{\frac{3}{2}}^{(2)} + \frac{1}{3|c|^3} Y_{\frac{3}{2}}^{(3)} \right], \\
p_2 &= Y_{\frac{3}{2}}^{(2)} \left[1 + \frac{4p_1}{|c|^3} + \frac{p_2}{4|c|^3} + \frac{112p_3}{81|c|^3} \right] \\
&= Y_{\frac{3}{2}}^{(2)} \left[1 + \frac{4}{|c|^3} Y_{\frac{3}{2}}^{(1)} + \frac{1}{4|c|^3} Y_{\frac{3}{2}}^{(2)} + \frac{112}{81|c|^3} Y_{\frac{3}{2}}^{(3)} \right], \\
p_3 &= Y_{\frac{3}{2}}^{(3)} \left[1 + \frac{p_1}{3|c|^3} + \frac{112p_2}{81|c|^3} + \frac{p_3}{8|c|^3} \right] \\
&= Y_{\frac{3}{2}}^{(2)} \left[1 + \frac{1}{3|c|^3} Y_{\frac{3}{2}}^{(1)} + \frac{112}{81|c|^3} Y_{\frac{3}{2}}^{(2)} + \frac{1}{8|c|^3} Y_{\frac{3}{2}}^{(3)} \right]. \qquad (12)
\end{aligned}$$

Or we can only keep the $1/|c|$ order as

$$p_r = Y_{\frac{3}{2}}^{(r)}, \qquad r = 1, 2, 3. \qquad (13)$$

and

$$p = p_1 + p_2 + p_3 \qquad (14)$$

is the equation of state. The low temperature thermodynamics can be studied via this equation in the whole parameter space. One can get the density n and compressibility κ from the equation of state from the formula $n = \partial p/\partial \mu$ and $\kappa = \partial^2 p/\partial \mu^2$ directly, which will be shown in the following sections.

III. THE SCALING FUNCTIONS OF THE PURE ZEEMAN SPLITTING CASE

The thermodynamics of this system is determined by the TBA equations, which are usually coupled nonlinear integrated equations. Thus the approximations are needed in the next step calculations [15]. The properties of 1D Fermi gases in the regime below crossover temperatures are described by Tomonaga-Luttinger liquid theory [14, 15]. However, in the critical regime, i.e. near the critical point and above the crossover temperatures, the correlation length tends to infinity and the second derivatives of free energy becomes divergent.

Thus it is difficult to study the properties near the critical point. In Zhou and Ho's work, the scaling function read off the critical exponents from thermodynamical properties at the quantum criticality. This provides a feasible way to study the critical properties in 1D systems. Guan and Ho applied this method to integrable strongly attractive Fermi gases with spin 1/2 to study the quantum criticality [24]. We will show that this method can be applied to the study of multi-component Fermi gases with strongly attractive interaction.

In the equal Zeeman splitting case, i.e., $H_1 = H_2$, the three-component problem can be reduced to two-component problem, i.e., only single fermions and neutral bound states exist, which is the simplest case of this problem. In former works [15], the specific heat of the strongly attractive Fermi gases can be expressed as

$$C_v \sim \left(\frac{1}{v_u} + \frac{1}{v_t}\right) \tag{15}$$

when equal Zeeman field is applied, where v_u and v_t are the velocity of unpaired fermions and trions, respectively. We can see that the strongly attractive Fermi gas with equal Zeeman splitting behaves like two-component Fermi gases with unpaired fermions and bound trions. This is a reminiscence of the properties of spin half Fermi gas. This suggests us use similar method to deal with the three-component problems when pure Zeeman splitting exists.

In order to study the quantum criticality, we need to work out the phase boundaries first. For simplicity, in the following calculation, we denote the unpaired fermions, pairs and trions as A, B, C, respectively. For instance, the mixture phase of trions and pairs are denoted as $B + C$ phase. By analyzing the band fillings at zero temperature, the phase boundaries can be obtained analytically from the TBA equations. There are three bands in the three-component problem, corresponding to the unpaired fermions, bound pairs and trions. For instance, near the boundary between C and $A + C$, the number single fermions is merely equal to zero, while the population of trions is still large. Thus on the boundary, there is $\varepsilon_1(0) = 0$ while $\varepsilon_3(Q_3) = 0$, where the integral boundary Q_3 of trion term is given by the Fermi surface, gives the integral boundary Q_3 of trion term, as shown in the phase boundary equations. Therefore, the phase boundary of this phase transition is expressed as

$$\mu_{c1} \;=\; -H_1 - \frac{1}{2\pi}\int_{-Q_3}^{Q_3} \frac{2|c|}{\lambda^2 + c^2}\varepsilon_3\left(\lambda\right) d\lambda, \tag{16}$$

where

$$\varepsilon_3(k) = 3\left(k^2-\mu-\frac{2c^2}{3}\right)-\frac{1}{2\pi}\int_{-Q_3}^{Q_3}\left[\frac{2|c|}{c^2+(k-\lambda)^2}+\frac{4|c|}{4c^2+(k-\lambda)^2}\right]\varepsilon_3(\lambda)\,d\lambda, \quad (17)$$

$$Q_3^2 = \mu+\frac{2c^2}{3}+\frac{1}{6\pi}\int_{-Q_3}^{Q_3}\left[\frac{2|c|}{c^2+\lambda^2}+\frac{4|c|}{4c^2+\lambda^2}\right]\varepsilon_3(\lambda)\,d\lambda. \quad (18)$$

The phase boundaries are determined by these coupled equations.

Similarly, the other three boundaries are

$$\mu_{c2} = -\frac{2c^2}{3}, \quad (19)$$

$$\mu_{c3} = -H_1, \quad (20)$$

$$\mu_{c4} = -\frac{2c^2}{3}-\frac{2|c|}{3\pi}\left[\sqrt{\mu_{c4}+H_1}-\frac{1}{|c|}\left(c^2+\mu_{c4}+H_1\right)\arctan\frac{\sqrt{\mu_{c4}+H_1}}{|c|}\right], \quad (21)$$

respectively.

In order to explore the method of calculating scaling functions, let's consider the simplest case–the phase boundary between the vacuum and phase C. From the equation of state (14), we can get the density of the system

$$n = 3Y_{\frac{1}{2}}^{(3)}\left(1-\frac{1}{|c|}Y_{\frac{1}{2}}^{(3)}\right). \quad (22)$$

Near the phase boundary, i.e., near the vacuum state, the pressure $p = p_3$ is very small. Thus it can be neglected during the calculation and the effective chemical potential $A^{(3)}$ which can be expressed in terms of μ and μ_c as

$$A^{(3)} \approx 3(\mu-\mu_c). \quad (23)$$

Here $\mu \approx \mu_c$, and $\mu_c = \mu_{c2} = -2c^2/3$, thus $A^{(3)}$ is very small. Therefore, the density can be approximately written in the universal scaling function form [10]

$$n(\mu,T) = n_0(\mu,T)+T^{\frac{d}{z}+1-\frac{1}{\nu z}}\mathcal{G}\left(\frac{\mu-\mu_c}{T^{\frac{1}{\nu z}}}\right), \quad (24)$$

where the background value $n_0 = 0$, the singular function

$$\mathcal{G} = -3\sqrt{\frac{3}{4\pi}}\mathrm{Li}_{\frac{1}{2}}(-e^{3(\mu-\mu_c)/T}), \quad (25)$$

and the critical components are $\frac{1}{\nu z} = 1$ and $\frac{d}{z}+1-\frac{1}{\nu z} = \frac{1}{2}$. For 1D systems, the dimension parameter $d = 1$, then it is easy to know that $z = 2$ and $\nu = \frac{1}{2}$ from the above algebraic

equations of critical components. The following results will show that in all cases the result of z and ν are the same, because the critical components are only determined by the symmetry of the Hamiltonian. The universal scaling form of Eq. (24) can be directly obtained from the equation of states $p = p_1 + p_2 + p_3$, where $p_{1,2,3}$ are given by Eq. (13). However, necessary approximations are needed in order to obtain the universal scaling form (24). Such approximations only involve the conditions $T \gg \mu - \mu_c$ and $T \ll c/n$ in low temperature expansions. In contrast, for $T \ll \mu - \mu_c$ and $T \ll c/n$, the Luttinger liquid thermodynamics is obtained. The explicit universal scaling forms of other thermodynamical quantities can be calculated in a similar way, see the compressibility Eq. (52) below.

Let's move to another representative case–the phase boundary between $A + C$ and C. In the strong coupling regime, the scaling function can be obtained under the series expansion and collecting terms up to $1/|c|$ orders. Near the critical point, we also have

$$A^{(3)} \approx 3\,(\mu - \mu_c) \tag{26}$$

by iteration of (17) and (18), collecting terms up to order $1/|c|$ and here $\mu_c = \mu_{c1}$.

In quantum critical regime of this phase, there are only a few trions, thus the pressure p_3 is small. From the expression of pressure, i.e., the equation of state (14), we know that $Y^{(3)}_{\frac{1}{2}}$ and $Y^{(3)}_{-\frac{1}{2}}$ are both small. Meanwhile, the number of pairs is relatively large. Thus by neglecting some small quantities, the result can be simplified and the scaling function is obtained as

$$n = n_0 + T^{\frac{1}{2}}\mathcal{G}\left(\frac{\mu - \mu_c}{T}\right), \tag{27}$$

where

$$n_0 = \frac{4}{\pi}a_{32}^{\frac{1}{2}}\left(1 + \frac{38}{27\pi|c|}a_{32}^{\frac{1}{2}}\right), \tag{28}$$

$$\mathcal{G}\left(\frac{\mu - \mu_c}{T}\right) = -3\sqrt{\frac{3}{4\pi}}\left(1 - \frac{32}{9\pi|c|}a_{32}^{\frac{1}{2}}\right)\mathrm{Li}_{\frac{1}{2}}\left(-e^{3(\mu-\mu_c)/T}\right). \tag{29}$$

Here the approximation

$$\mathrm{Li}_s\left(-e^u\right) \approx -\frac{u^s}{\Gamma(s+1)} \tag{30}$$

has been applied in the above calculation, and $a_{12} = c^2/4 - H_1 + H_2/2$ and $a_{32} = -5c^2/12 + H_2/2$. In this scaling function, n_0 is the contribution from the background, i.e., the contribution from the cluster which don't experience a sudden change as the driving parameter varies across the phase boundaries.

Similarly, the compressibility can be written in the form

$$\kappa - \kappa_0 = T^{-\frac{1}{2}} \mathcal{G}' \left(\frac{\mu - \mu_c}{T} \right), \tag{31}$$

where

$$\kappa_0 = \frac{2}{\pi} a_{32}^{-\frac{1}{2}} \left(1 + \frac{178}{27\pi|c|} a_{32}^{\frac{1}{2}} \right), \tag{32}$$

$$\mathcal{G}' \left(\frac{\mu - \mu_c}{T} \right) = -9\sqrt{\frac{3}{4\pi}} \left(1 - \frac{32}{3\pi|c|} a_{32}^{\frac{1}{2}} \right) \mathrm{Li}_{-\frac{1}{2}} \left(-e^{3(\mu-\mu_c)/T} \right). \tag{33}$$

Here we can easily see that the critical parameters are still $z = 2$ and $\nu = \frac{1}{2}$.

In general, in the quantum liquid phases of 1D many-body systems, the equation of states can be written in terms of polylogarithm functions. Quantum criticality describes universal scaling behavior of thermodynamics near the critical points. In a small window near a critical point, the polylogarithm functions capture proper thermal and quantum fluctuations so that correct critical correct critical exponents can be mapped out from the scaling forms written in terms of polylogarithm functions. However, the Sommerfeld expansions with the equation of states only lead to some terms involving the powers of temperature, which are not enough to capture such strong thermal and quantum fluctuations. Therefore, the Luttinger liquid physics does not contain the critical behavior in the quantum critical regime.

IV. THE GENERAL CASE: THE SCALING FUNCTIONS AT ARBITRARY PHASE BOUNDARIES

In last section, we successfully solve the equal Zeeman splitting case using the method for the spin-half problem. Similarly, we can also apply this method to solve unequal Zeeman splitting cases even for the whole parameter plane. We can see that the phase boundary is determined by μ, H_1 and H_2. Thus it is possible to give the general phase boundary equations and the scaling functions.

A. The analytical phase boundaries of different phases in $\mu - H$ plane

The above method can also be applied to all the phase boundaries in this problem. Without loss of generality, we consider the three states co-exist case–the phase boundary between $A + C$ and $A + B + C$. Near the phase boundary, the particle number of B is small

and those of A and C are relatively large, hence we have $\varepsilon_1(Q_1)=0$, $\varepsilon_3(Q_3)=0$, $\varepsilon_2(0)=0$, where Q_1 and Q_3 are the integral boundaries of ε_1 and ε_3, respectively. Thus the phase boundary is expressed as

$$\mu_c=-\frac{c^2}{4}-\frac{H_2}{2}-\frac{1}{4\pi}\int_{-Q_1}^{Q_1}\frac{|c|}{\frac{c^2}{4}+\lambda^2}\,\varepsilon_1(\lambda)\,d\lambda-\frac{1}{4\pi}\int_{-Q_3}^{Q_3}\left[\frac{|c|}{\frac{c^2}{4}+\lambda^2}+\frac{3|c|}{\frac{9c^2}{4}+\lambda^2}\right]\varepsilon_3(\lambda)\,d\lambda. \quad (34)$$

where the ε_1 and ε_3 are determined by the simplified TBA equations

$$\varepsilon_1(k) = k^2-\mu-H_1-\frac{1}{2\pi}\int_{-Q_3}^{Q_3}\frac{2|c|}{c^2+\lambda^2}\,\varepsilon_3(\lambda)\,d\lambda, \quad (35)$$

$$\varepsilon_3(k) = 3k^2-3\mu-2c^2-\frac{1}{2\pi}\int_{-Q_1}^{Q_1}\frac{2|c|}{c^2+\lambda^2}\,\varepsilon_1(\lambda)\,d\lambda - \frac{1}{2\pi}\int_{-Q_3}^{Q_3}\left[\frac{2|c|}{c^2+\lambda^2}+\frac{4|c|}{4c^2+\lambda^2}\right]\varepsilon_3(\lambda)\,d\lambda, \quad (36)$$

respectively, and the integral boundaries Q_1 and Q_3 satisfy equations

$$Q_1^2 = \mu+H_1+\frac{1}{2\pi}\int_{-Q_3}^{Q_3}\frac{2|c|}{c^2+\lambda^2}\,\varepsilon_3(\lambda)\,d\lambda, \quad (37)$$

$$Q_3^2 = \mu+\frac{2c^2}{3}+\frac{1}{6\pi}\int_{-Q_1}^{Q_1}\frac{|c|}{c^2+\lambda^2}\,\varepsilon_1(\lambda)\,d\lambda+\frac{1}{6\pi}\int_{-Q_3}^{Q_3}\left[\frac{2|c|}{c^2+\lambda^2}+\frac{4|c|}{4c^2+\lambda^2}\right]\varepsilon_3(\lambda)\,d\lambda \quad (38)$$

The Eqs. (34)–(38) determine the boundary of phase transition from $A+C$ to $A+B+C$ together. The last two terms of (34) are the effect of the background A and C components, respectively. This is the general method to calculate all the phase boundaries, and can be applied for such quantum Fermi gases with $SU(N)$ symmetry when N is an arbitrary integer.

B. The universal case of quantum criticality–scaling functions and phase diagrams

Now let's calculate the scaling function of the phase transition from A+C to A+B+C.

The total density and compressibility are

$$n = Y^{(1)}_{\frac{1}{2}}\left(1-\frac{4}{|c|}Y^{(2)}_{\frac{1}{2}}-\frac{2}{|c|}Y^{(3)}_{\frac{1}{2}}\right)+2Y^{(2)}_{\frac{1}{2}}\left(1-\frac{2}{|c|}Y^{(1)}_{\frac{1}{2}}-\frac{1}{|c|}Y^{(2)}_{\frac{1}{2}}-\frac{8}{3|c|}Y^{(3)}_{\frac{1}{2}}\right) +3Y^{(3)}_{\frac{1}{2}}\left(1-\frac{2}{3|c|}Y^{(1)}_{\frac{1}{2}}-\frac{16}{9|c|}Y^{(2)}_{\frac{1}{2}}-\frac{1}{|c|}Y^{(3)}_{\frac{1}{2}}\right) \quad (39)$$

and

$$\kappa = Y^{(1)}_{-\frac{1}{2}}\left(1-\frac{12}{|c|}Y^{(2)}_{\frac{1}{2}}-\frac{6}{|c|}Y^{(3)}_{\frac{1}{2}}\right)+4Y^{(2)}_{-\frac{1}{2}}\left(1-\frac{6}{|c|}Y^{(1)}_{\frac{1}{2}}-\frac{3}{|c|}Y^{(2)}_{\frac{1}{2}}-\frac{8}{|c|}Y^{(3)}_{\frac{1}{2}}\right) +9Y^{(3)}_{-\frac{1}{2}}\left(1-\frac{2}{|c|}Y^{(1)}_{\frac{1}{2}}-\frac{16}{3|c|}Y^{(2)}_{\frac{1}{2}}-\frac{3}{|c|}Y^{(3)}_{\frac{1}{2}}\right), \quad (40)$$

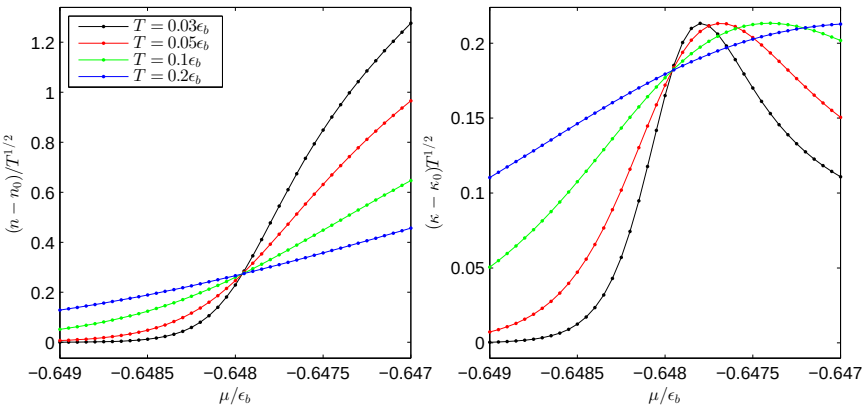


FIG. 1: The left figure shows the scaled density n vs chemical potential μ; the right one shows scaled compressibility κ vs chemical potential μ for the phase transition from vacuum to B. In this case, $n_0 = \kappa_0 = 0$. The magnetic fields are set for equal Zeeman splitting $H_1 = H_2 = 1.32\epsilon_b$. Here we define $\epsilon_b = c^2/2$. The curves in each figure are set for $T = 0.03\epsilon_b, 0.05\epsilon_b, 0.1\epsilon_b, 0.2\epsilon_b$.

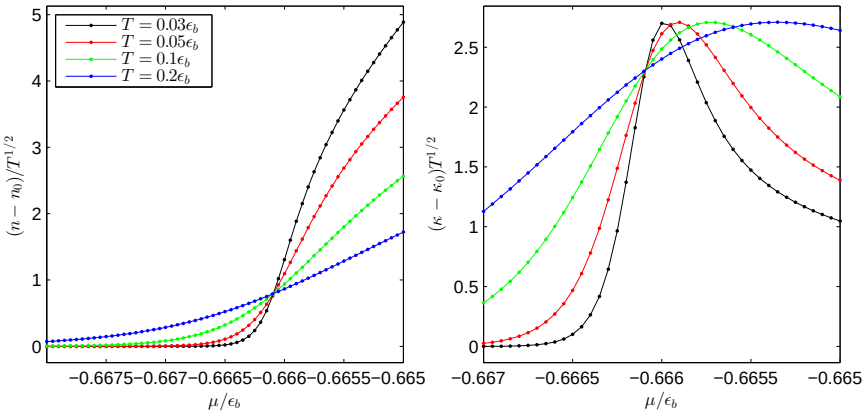


FIG. 2: The left figure shows the scaled density n vs chemical potential μ; the right one shows scaled compressibility κ vs chemical potential μ at $T = 0.03\epsilon_b, 0.05\epsilon_b, 0.1\epsilon_b, 0.2\epsilon_b$ for the phase transition from B to $B + C$. In this case, $n_0 \neq 0$, $\kappa_0 \neq 0$. The magnetic fields are set for equal Zeeman splitting $H_2 = 2H_1 = 1.7\epsilon_b$.

respectively.

In the limit of $T \to 0$, $\mu \to \mu_c$, n and $T > |\mu - \mu_c|$. Thus κ can be cast into universal form. Since the $\mu - \mu_c$ terms are much less than the other quantities, we can keep the zeroth

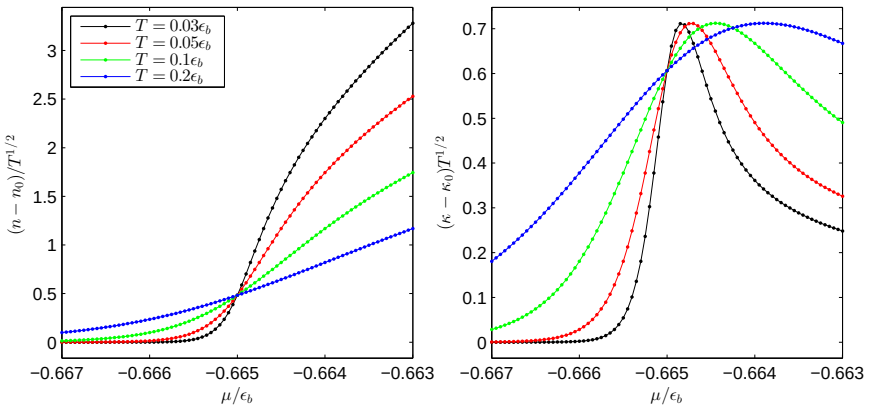


FIG. 3: The left figure shows the scaled density n vs chemical potential μ; the right one shows scaled compressibility κ vs chemical potential μ at $T = 0.03\epsilon_b, 0.05\epsilon_b, 0.1\epsilon_b, 0.2\epsilon_b$ for the phase transition from $A + C$ to $B + C$. In this case, $n_0 \neq 0$, $\kappa_0 \neq 0$. The magnetic fields are set for unequal Zeeman splitting $H_2 = 1.2H_1$, $H_1 = 1.34\epsilon_b$.

order of $Y^{(2)}_{\frac{1}{2}}$ and neglect the first order terms and simplify the $Y^{(1)}_{\frac{1}{2}}$ and $Y^{(3)}_{\frac{1}{2}}$ terms as follows

$$Y^{(1)}_{\frac{1}{2}} \approx \frac{1}{\pi}\sqrt{a_u}, \qquad Y^{(1)}_{-\frac{1}{2}} \approx \frac{1}{2\pi}\sqrt{\frac{1}{a_u}}, \tag{41}$$

$$Y^{(3)}_{\frac{1}{2}} \approx \frac{1}{\pi}\sqrt{3a_t}, \qquad Y^{(3)}_{-\frac{1}{2}} \approx \frac{1}{2\pi}\sqrt{\frac{3}{a_t}}, \tag{42}$$

where

$$a_u = a_{21}\left(1 + \frac{16}{3\pi|c|}a_{21}^{\frac{1}{2}}\right) - \frac{32}{9\pi|c|}a_{23}^{\frac{3}{2}}, \tag{43}$$

$$a_t = 3a_{23}\left(1 + \frac{10}{3\pi|c|}a_{23}^{\frac{1}{2}}\right) - \frac{8}{3\pi|c|}a_{21}^{\frac{3}{2}}, \tag{44}$$

and $a_{21} = -c^2/4 + H_1 - H_2/2$ and $a_{23} = 5c^2/12 - H_2/2$.

Thus we have

$$n - n_0 = T^{\frac{1}{2}}\mathcal{G}\left(\frac{\mu - \mu_c}{T}\right), \tag{45}$$

and

$$\kappa - \kappa_0 = T^{-\frac{1}{2}}\mathcal{G}'\left(\frac{\mu - \mu_c}{T}\right), \tag{46}$$

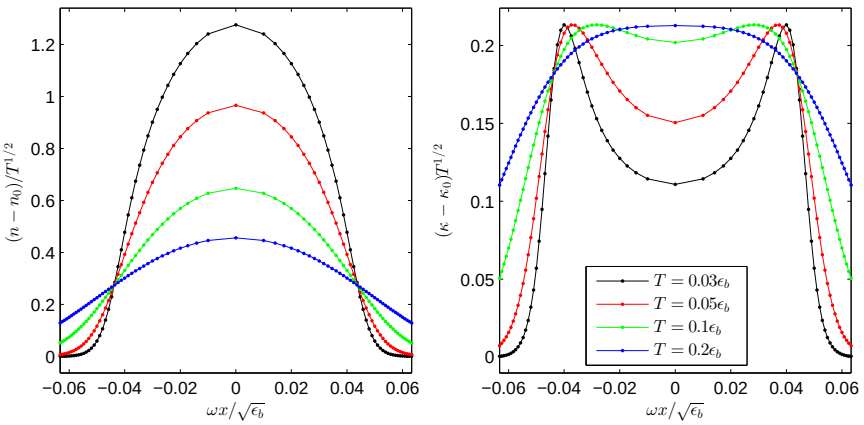


FIG. 4: Quantum criticality can be mapped out by the measurement of local values of thermodynamics in a harmonic trap. The left panel shows the local density $n(x)$ vs dimensionless position ωx for the phase transition from vacuum into the phase B at $T = 0.03\epsilon_b, 0.05\epsilon_b, 0.1\epsilon_b, 0.2\epsilon_b$. Whereas the right one shows the local compressibility $\kappa(x)$ vs ωx at the same temperatures $T = 0.03\epsilon_b, 0.05\epsilon_b, 0.1\epsilon_b, 0.2\epsilon_b$. Here numerical settings are $\mu_0 = -0.647\epsilon_b$ and $H_1 = H_2 = 1.32\epsilon_b$. For this phase transition, the regular parts of the density and compressibility are both zero. From proper temperature-scaled density and compressibility, one reads off the critical exponents $Z = 2$ and $\nu = 1/2$. With such exponents, the density and compressibility indeed show the intersection nature at the critical point.

where

$$n_0 = \frac{\sqrt{a_u}}{\pi}\left(1-\frac{2\sqrt{3}}{\pi|c|}\sqrt{a_t}\right)+\frac{3\sqrt{3}}{\pi}\sqrt{a_t}\left(1-\frac{2}{3\pi|c|}\sqrt{a_u}-\frac{\sqrt{3}}{\pi|c|}\sqrt{a_t}\right), \quad (47)$$

$$\mathcal{G}\left(\frac{\mu-\mu_c}{T}\right) = -\sqrt{\frac{2}{\pi}}\left(1-\frac{2}{\pi|c|}\sqrt{a_u}-\frac{8\sqrt{3}}{3\pi|c|}\sqrt{a_t}\right)\mathrm{Li}_{\frac{1}{2}}\left(-e^{2(\mu-\mu_c)/T}\right), \quad (48)$$

and

$$\kappa_0 = \frac{1}{2\pi\sqrt{a_u}}\left(1-\frac{6\sqrt{3}}{\pi|c|}\sqrt{a_t}\right)+\frac{9\sqrt{3}}{2\pi\sqrt{a_t}}\left(1-\frac{2}{\pi|c|}\sqrt{a_u}-\frac{3\sqrt{3}}{\pi|c|}\sqrt{a_t}\right), \quad (49)$$

$$\mathcal{G}'\left(\frac{\mu-\mu_c}{T}\right) = -2\sqrt{\frac{2}{\pi}}\left(1-\frac{6}{\pi|c|}\sqrt{a_u}-\frac{8\sqrt{3}}{\pi|c|}\sqrt{a_t}\right)\mathrm{Li}_{-\frac{1}{2}}\left(-e^{2(\mu-\mu_c)/T}\right). \quad (50)$$

Compare with the first case, we can see the difference in the background: state B is added from vacuum phase in the first case and in this case it is added from $A + C$ phase. The first and second terms of n_0 and κ_0 are the contributions from unpaired fermions and

trions, respectively. The a_u and a_t terms in $\mathcal{G}$ and $\mathcal{G}'$ are the contributions from A and C, respectively. Again we can see that the critical parameters are still $z = 2$ and $\nu = \frac{1}{2}$. From the scaling functions of n and κ we have calculated above, we can plot the scaled diagrams of $\left[(n - n_0)/\sqrt{T}\right] - \mu$ and $\left[(\kappa - \kappa_0)\sqrt{T}\right] - \mu$, see Fig. 1-Fig. 3. The diagrams show that the curves intersect at the critical point. The cross point gives one point on the boundary between two different phases. This method map out the phase diagrams of homogeneous systems through the trapped ultracold atoms in experiments.

In the trapped gas, the local chemical potential μ is replaced by $\mu(x) = \mu_0 - \frac{1}{2}m\omega^2 x^2$. Within the local density approximation, the quantum criticality can be mapped out from the trapped gas at finite temperatures. For example, for the phase transitions from vacuum to B, the quantum criticality of density and compressibility can be mapped out by the measurement of the the local values, see Fig 4. Similar study can be carried out for other critical regions.

The phase diagrams at finite temperatures can also be achieved from the equation of state, see Fig. 5. From this figure we see that one can control two external fields H_1 and H_2 trigger multiple critical points. So that one can have phase transition from one cluster state into multiple cluster states, for example from phase B into the phase $A + B + C$, as the chemical potential increase across the multiple critical point. Here the scaling function of thermodynamics involves the background of B states and the singular part consisting of three cluster states. This method is also universal and can be applied to Fermi gases with arbitrary $SU(N)$ symmetry.

V. CONCLUSION

In conclusion, polylogarithm functions have been applied to study the quantum critical behavior of 1D strongly attractive three-component Fermi gas with both linear and nonlinear Zeeman splitting at low temperatures via thermodynamic Bethe ansatz equations (2) to (6). The equation of state, phase boundaries and scaling functions have been derived analytically in terms of interaction strength $1/|c|$. From the scaling functions, the phase diagrams at zero temperature for homogeneous systems can be mapped out from the inhomogeneous trapping systems at finite temperatures. The general forms of quantum criticality (51) and (52) can be written in terms of the multiple changes of cluster states either in regular part or

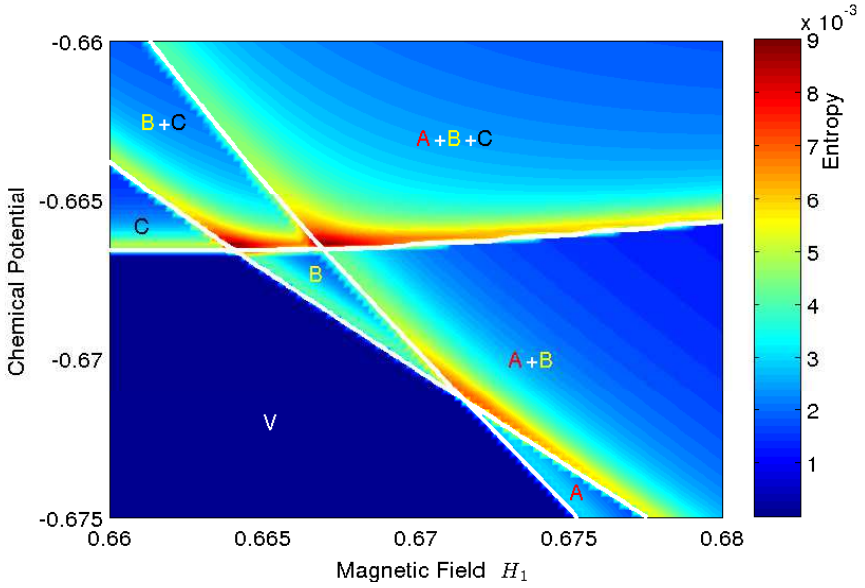


FIG. 5: The phase diagram of the entropy S in $\mu - H_1$ plane for temperature $T = 0.001\epsilon_b$. Here $H_2 = 1.255H_1$. The white lines show the phase boundaries at $T = 0$, see Section III.

in singular part. For example the density and compressibility can be cast into the following general forms

$$n - n_0 = T^{\frac{1}{2}}\mathcal{G}\left(\tfrac{\mu-\mu_c}{T}\right), \quad \mathcal{G}(x) = -\sum_{j=1}^{N} \tfrac{r_j^{3/2}}{2\sqrt{\pi}}\lambda_j \mathrm{Li}_{1/2}(-\mathrm{e}^{r_j x}), \tag{51}$$

$$\kappa - \kappa_0 = T^{-\frac{1}{2}}\mathcal{G}'\left(\tfrac{\mu-\mu_c}{T}\right), \mathcal{G}'(x) = -\sum_{j=1}^{N} \tfrac{r_j^{5/2}}{2\sqrt{\pi}}\lambda'_j \mathrm{Li}_{-1/2}(-\mathrm{e}^{r_j x}), \tag{52}$$

where the background density n_0, compressibility κ_0 involve the constant parts of these quantities which only depend on the critical effective magnetic fields and chemical potentials, r_j are the particle effective masses of the corresponding classters with the sudden change of the density of the states, λ_j are some constants and the addition is taken over all the driven strings. When the background of the phase transition is the vacuum state, $\lambda_j = 1$.

Whereas the scaling functions of the singular parts $\mathcal{G}$ and $\mathcal{G}'$ are uniquely determined by a sudden change of density of state of the single and/or cluster states. For example, Eqs. (47)-(50) near the phase transition from $A+C$ to $A+B+C$ illustrate the case involving the sudden change of the density of state of the two-atom cluster states. However, for the phase transition from phase B to $A+B+C$, the scaling function involves two parts related to the sudden change of density of state of the single fermions and three-body cluster states, see Fig. 5. The phase diagram at the zero temperature can be mapped out from the trapped

gas at finite temperatures with quantum criticality. This method is in general valid for 1D continuous Fermi gases and can be applied to study the universal quantum criticality of strongly attractive Fermi gases with high spin symmetries. As an obvious example, the general $SU(N)$ case can be well studied via this method. Moreover, the far-from equilibrium universal dynamics of one dimensional interacting fermions with large spin symmetries is particularly interesting. One can expect that the non-equilibrium states of the large spin systems crossing of a phase transition are described by the Kibble-Zurek mechanism, see a recent review [40]. Integrable models out of equilibrium crossing quantum phase transitions would provide practicable settings for the Kibble-Zurek mechanism.

Acknowledgments

This work is in part supported by the National Basic Research Program of China under Grant number 2012CB922101 and NSFC under Grant number 11374331 and 11304357, the Knowledge Innovation Project of Chinese Academy of Sciences and the Australian Research Council. The authors thank Prof. Yupeng Wang for helpful discussion.

[1] Subir Sachdev, *Quantum Phase Transitions* (Cambridge University Press, Cambridge, 1999).

[2] R. Coldea, et al. Science **327**, 177 (2010).

[3] J.A.Hertz, Phys. Rev. B **14**, 1165 (1976).

[4] K. G. Wilson, Phys. Rev. B **4**, 3174 (1971); Phys. Rev. B **4**, 3184 (1971).

[5] T. Senthil, Phys. Rev. B **70**, 144407 (2004).

[6] M. P. A. Fisher, P. B. Weichman, G. Grinstein and D. F. Fisher, Phys. Rev. B **40**, 546 (1989).

[7] Sean A. Hartnoll, Lectures on holographic methods for condensed matter physics, Class. Quant. Grav. **26**, 224002 (2009).

[8] C. P. Herzog, Lectures on holographic superfluidity and superconductivity, J. Phys. A: Math. Theor. **42**, 343001 (2009).

[9] A.S.T. Pires, AdS/CFT correspondence in condensed matter, arXiv: 1006.5838v1.

[10] Qi Zhou and Tin-Lun Ho, Phys. Rev. Lett. 105, 245702 (2010).

[11] T.-L. Ho and Q. Zhou, Nature Physics, **6**, 131 (2010).

[12] X. W. Guan, M. T. Batchelor, C. Lee, and M. Bortz, Phys. Rev. B **76**, 085120 (2007).

[13] X.-W. Guan, J.-Y. Lee, M. T. Batchelor, X. G. Yin and S. Chen, Phys. Rev. A **82**, 021606(R) (2010).

[14] E. Zhao, X.-W. Guan, W. Vincent Liu, M. T. Batchelor, and M. Oshikawa, Phys. Rev. Lett. **103**, 140404 (2009)

[15] Peng He, Xiangguo Yin, Xiwen Guan, Murray Batchelor and Yupeng Wang, Phys. Rev. A **82**, 053633 (2010).

[16] J. Cao, Y. Jiang and Y. Wang, Europhys. Lett. **79**, 30005 (2007).

[17] J. Y. Lee, X.-W. Guan, M. T. Batchelor and C. Lee, Phys. Rev. A **80**, 063625 (2009).

[18] G. V. Shlyapnikov and A. M. Tsvelik, New J. Phys. **13**, 065012 (2011).

[19] C. C. N. Kuhn, X. W. Guan, A. Foerster, and M. T. Batchelor, Phys. Rev. A **85**, 043606 (2012);

C. C. N. Kuhn, X. W. Guan, A. Foerster, and M. T. Batchelor, Phys. Rev. A **86**, 011605(R) (2012).

[20] M. A. Cazalilla, A. M. Rey, arXiv:1403:2792.

[21] S. Taie *et al.*, Phys. Rev. Lett. **105**, 190401 (2010).

[22] S. Taie *et al.*, Nature Phys. **8**, 825 (2012).

[23] G. Pagano *et al.* Nature Physics, **10**, 198 (2014).

[24] Xiwen Guan and Tin-Lun Ho, Phys. Rev. A **84**, 023616 (2011).

[25] Xi-Wen Guan and Murray T. Batchelor, J. Phys. A: Math. Theor. **44**, 102001 (2011).

[26] Xiangguo Yin, Xi-Wen Guan, Yunbo Zhang, Shu Chen, Phys. Rev. A 85, 013608 (2012).

[27] Xiangguo Yin, Xi-Wen Guan, Shu Chen, Murray T Batchelor, Phys. Rev. A 84, 011602(R) (2011).

[28] X.-W. Guan, M. T. Batchelor and C. Lee, Rev. Mod. Phys. **85**, 1633 (2013).

[29] C. C. N. Kuhn and A. Foerster, New J. Phys. 14, 013008 (2012).

[30] P. Schlottmann, J. Phys.: Condens. Matter **5** (1993) 5869;

P. Schlottmann, J. Phys.: Condens. Matter **6** (1994) 1359.

[31] P. Schlottmann and A. A. Zvyagin, Phys. Rev. B **85**, 205129 (2012);

P. Schlottmann and A. A. Zvyagin Phys. Rev. B **85**, 024535 (2012).

[32] X.-W. Guan, M. T. Batchelor, C. Lee and H.-Q. Zhou, Phys. Rev. Lett. **100**, 200401 (2008).

[33] Y. Liao, A. Rittner, T. Paprotta, W. Li, G. Patridge, R. Hulet, S. Baur, and E. Mueller,

Nature **467**, 567 (2010).

[34] B. Sutherland, Phys. Rev. Lett. **20**, 98 (1968).

[35] M. Takahashi, Prog. Theor. Phys. **44**, 899 (1970).

[36] M. Takahashi, *Thermodynamic of One-Dimensional Solvable Models* (Cambridge University Press, Cambridge, 1999).

[37] M. T. Batchelor, X.-W. Guan, N. Oelkers and Z. Tsuboi, Adv. Phys. **56**, 465 (2007).

[38] P. Lecheminant, E. Boulat and P. Azaria, Phys. Rev. Lett. **95**, 240402 (2005).

[39] Y. Maeda, C. Hotta and M. Oshikawa, Phys. Rev. Lett. **99**, 057205 (2007).

[40] A. del Campo and W. H. Zurek, Int. J. Mod.Phys. A **29**, 1430018 (2014).